Prognostics Approach for Power MOSFET under Thermal-Stress Aging

José R. Celaya, PhD, SGT Inc., Prognostics Center of Excellence, NASA Ames Research Center
Abhinav Saxena, PhD, SGT Inc., Prognostics Center of Excellence, NASA Ames Research Center
Chetan S. Kulkarni, ISIS, Vanderbilt University
Sankalita Saha, PhD, MCT., Prognostics Center of Excellence, NASA Ames Research Center
Kai Goebel, PhD, Prognostics Center of Excellence, NASA Ames Research Center

Key Words: Power MOSFET, Prognostics, PHM, Accelerated Life Test

SUMMARY & CONCLUSIONS

The prognostic technique for a power MOSFET presented in this paper is based on accelerated aging of MOSFET IRF520Npbf in a TO-220 package. The methodology utilizes thermal and power cycling to accelerate the life of the devices. The major failure mechanism for the stress conditions is die-attachment degradation, typical for discrete devices with lead-free solder die attachment. It has been determined that die-attach degradation results in an increase in ON-state resistance due to its dependence on junction temperature. Increasing resistance, thus, can be used as a precursor of failure for the die-attach failure mechanism under thermal stress. A feature based on normalized ON-resistance is computed from *in-situ* measurements of the electro-thermal response. An Extended Kalman filter is used as a model-based prognostics techniques based on the Bayesian tracking framework.

The proposed prognostics technique reports on preliminary work that serves as a case study on the prediction of remaining life of power MOSFETs and builds upon the work presented in [1]. The algorithm considered in this study had been used as prognostics algorithm in different applications and is regarded as suitable candidate for component level prognostics. This work attempts to further the validation of such algorithm by presenting it with real degradation data including measurements from real sensors, which include all the complications (noise, bias, etc.) that are regularly not captured on simulated degradation data.

The algorithm is developed and tested on the accelerated aging test timescale. In real world operation, the timescale of the degradation process and therefore the RUL predictions will be considerable larger. It is hypothesized that even though the timescale will be larger, it remains constant through the degradation process and the algorithm and model would still apply under the slower degradation process. By using accelerated aging data with actual device measurements and real sensors (no simulated behavior), we are attempting to assess how such algorithm behaves under realistic conditions.

1 INTRODUCTION

Prognostics is an engineering discipline focused on predicting the time at which an in-service component will fail. The science of prognostics is based on the analysis of failure modes, detection of early signs of wear and aging, and fault conditions. These signs are then correlated with a damage propagation model and suitable prediction algorithms to arrive at a "remaining useful life" (RUL) estimate. The discipline that links studies of failure mechanisms to system lifecycle management is often referred to as prognostics and health management (PHM). Power semiconductor devices such as MOSFETs (Metal Oxide Field Effect Transistors) are essential components of electronic and electrical subsystems in on-board autonomous functions for vehicle controls, communications, navigation, and radar systems. In current practices, maintenance schedules are usually based on reliability data available from the manufacturer. However, while this approach works well in aggregate on a large number of components, failures on individual components are not necessarily averted. For mission critical systems it is extremely important to avoid such failures. This calls for condition based prognostic health management methods.

1.1 Related Work

In [2] a model-based prognostics approach for discrete IGBTs was presented. RUL predictions were accomplished using a particle filter algorithm where the collector-emitter leakage current was used as the primary precursor of failure. A prognostics approach for power MOSFETs was presented in [3], where, the threshold voltage was used as a precursor of failure; a particle filter was used in conjunction with an empirical degradation model.

Identification of parameters that indicate precursors to failure in discrete power MOSFETs and IGBTs have received considerable attention in recent years. Several studies have focused on precursor of failure parameters for discrete IGBTs under thermal degradation due to power cycling overstress. In

[4], collector-emitter voltage was identified as a health indicator; in [5], the maximum peak of the collector-emitter ringing at turn OFF transient was identified as the degradation variable; in [6] the switching turn-OFF time was recognized as failure precursor; and switching ringing was used in [7] to characterize degradation. For discrete power MOSFETs, ON-resistance was identified as a precursor of failure for the die-solder degradation failure mechanism [8, 9]. A shift in threshold voltage was identified as failure precursor due to gate structure degradation fault mode [10].

There have been some efforts in the development of degradation models that are a function of the usage/aging time based on accelerated life test. For example, empirical degradation models for model-based prognostics are presented in [2] and [3] for discrete IGBTs and power MOSFET respectively. Gate structure degradation modeling of discrete power MOSFETs under ion impurities has been presented in [11].

2 ACCELERATED LIFE EXPERIMENTS

The development of prognostics algorithms face similar constrains as reliability engineering in that both need information about failure events of critical electronics systems. These data are is rarely ever available. In addition, prognostics requires information about the degradation process leading to an irreversible failure; therefore, it is necessary to record *in-situ* measurements of key output variables and observable parameters in the accelerated aging process in order to develop and learn failure progression models.

Thermal cycling overstress leads to thermo-mechanical stresses in electronics due to mismatch of the coefficient of thermal expansion between different elements in the component's packaged structure. The accelerated aging applied to the devices presented in this work consists of thermal overstress. Latch-up, thermal run-away, or failure to turn ON due to loss of gate control are considered as failure conditions. Thermal cycles were induced by power cycling the devices without the use of an external heat sink. The device case temperature was measured and directly used as control variable for the thermal cycling application. For power cycling, the applied gate voltage was a square wave signal with an amplitude of ~15V, a frequency of 1KHz and a duty cycle of 40%. The drain-source was biased at 4Vdc and a resistive load of 0.2Ω was used on the collector side output of the device. The aging system used for these experiments is described in [5], and the accelerated aging methodology is presented in [8].

In-situ measurements of the drain current (I_D) and the drain to source voltage (V_{DS}) are recorded as the device is under aging regime. The ON-state resistance $R_{DS(ON)}$ in this application was computed as the ratio of V_{DS} and I_D on the ON-state of the square waveform. In the accelerated aging system, it is not possible to measure junction temperature directly, as a result, the increase in junction temperature is observed by monitoring the increase in $R_{DS(ON)}$. Furthermore, junction temperature is also a function of the case temperature, which is measured and recorded *in-situ*. Therefore, the measured $R_{DS(ON)}$ was normalized to eliminate the case temperature effects and reflect only changes due to degradation. Due to manufacturing variability, the pristine condition $R_{DS(ON)}$ varies from device to device. In order to take this into account, the normalized $R_{DS(ON)}$ time series is shifted by applying a bias factor representing the pristine condition value. The resulting trajectory ($\Delta R_{DS(ON)}$) from pristine condition to failure, represents the degradation process due to die-attach failure and represents the increase in $R_{DS(ON)}$ through the aging process.

These measurements do not have a fixed sampling rate. On average, there is a transient response measurement every 400 ns. This consists of a snapshot of the transient response which includes one full square waveform cycle. Therefore a resampling of the curve was carried out to have uniform sampling and a reduced sampling frequency on the failure precursor trajectory. The signals were filtered by computing the mean of every one minute long window. There are six available aged MOSFETs under thermal overstress. Figure 1 presents the $\Delta R_{DS(ON)}$ trajectories for the six cases.

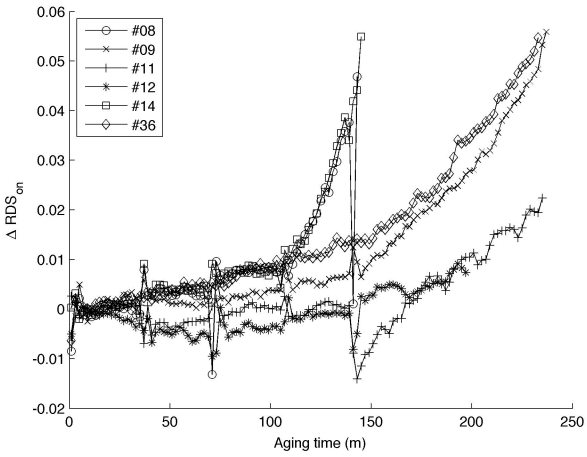

Figure 1. $\Delta R_{DS(ON)}$ trajectories for all MOSFETs.

3 DEGRADATION MODELING

An empirical degradation model is suggested based on the degradation process observed on $\Delta R_{DS(ON)}$ for the six aged devices. It can be seen that this process grows exponentially as a function of time and that the exponential behavior starts at different points in time for different devices. An empirical degradation model can be used to model the degradation process when a physics-based degradation model is not available. This methodology has been used for prognostics of electrolytic capacitors using a Kalman filter [12]. There, the exponential degradation model was posed as a linear first-order discrete dynamic system in the form of a state-space model representing the dynamics of the degradation process. The proposed degradation model for the power MOSFET application is defined as follows. Let $R = \Delta R_{DS(ON)}$ be the increase in ON-resistance due to aging.

$$R = \alpha\left(e^{\beta \cdot t} - 1\right), \tag{1}$$

where t is time and α and β are model parameters that could be static or estimated on-line as part of the Bayesian tracking framework. This model structure is capable of representing the exponential behavior of the degradation process for the different devices. Table 1 presents parameter estimation results for model (1) based on non-linear least-squares estimation. The estimate for both parameters is presented along with their corresponding sample variance. It is clearly observed that the parameters of the model will be different for different devices. Therefore, the parameters α and β need to be estimated online in order to ensure accuracy. Figure 2 presents the estimation results for device #36.

Device	$\hat{\alpha}$	$\hat{\beta}$	σ_{α}^2	σ_{β}^2
#08	$3.70\text{x}10^{-4}$	$3.24\text{x}10^{-2}$	$1.01\text{x}10^{-8}$	$4.27\text{x}10^{-6}$
#09	$7.92\text{x}10^{-4}$	$1.79\text{x}10^{-2}$	$3.50\text{x}10^{-9}$	$1.18\text{x}10^{-7}$
#11	$6.00\text{x}10^{-6}$	$3.56\ \text{x}10^{-2}$	$1.10\ \text{x}10^{-11}$	$6.20\ \text{x}10^{-6}$
#12	$9.75\ \text{x}10^{-7}$	$4.70\ \text{x}10^{-2}$	$9.75\ \text{x}10^{-7}$	$4.70\ \text{x}10^{-2}$
#14	$2.60\text{x}10^{-4}$	$3.60\text{x}10^{-2}$	$1.64\text{x}10^{-9}$	$-4.71\text{x}10^{-9}$
#36	$2.67\text{x}10^{-3}$	$1.31\text{x}10^{-2}$	$1.02\text{x}10^{-8}$	$2.99\text{x}10^{-8}$

Table 1. Static parameter estimation results for degradation model in equation (1) applied to degradation data in Figure 1.

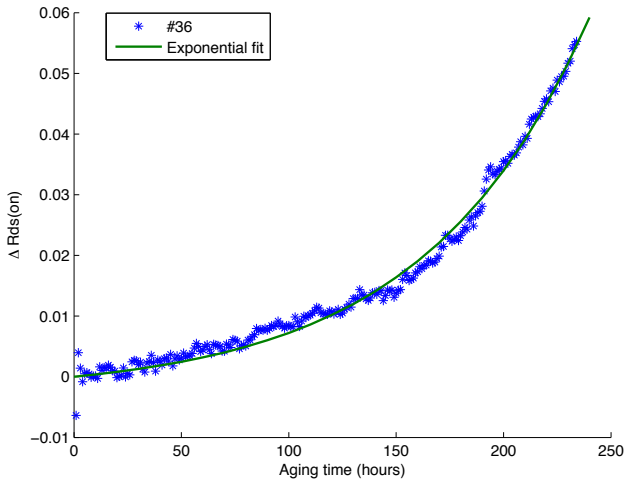

Figure 2. Non-linear least squares for device #36.

3.1 Dynamic degradation model for Bayesian tracking

The degradation model presented in equation (1) is converted into a dynamic model in order to obtain the state-space representation needed for Bayesian tracking. Defining the parameters α and β be time dependent parameters, then the derivative of (1) is given by,

$$\dot{R} = \alpha e^{\beta t}\left(\beta + t\,\dot{\beta}\right) + e^{\beta t}\dot{\alpha} - \dot{\alpha}\,. \tag{2}$$

Defining $\dot{\alpha} = 0$ and $\dot{\beta} = 0$, the dynamic model representation is given by,

$$\begin{aligned} \dot{R} &= (R + \alpha)(\beta), \\ \dot{\alpha} &= 0, \\ \dot{\beta} &= 0. \end{aligned} \tag{3}$$

In this model, α and β are also state variables that change through time. Therefore, the model is a non-linear dynamic system and Bayesian tracking algorithms like the extended Kalman or particle filters are needed for on-line state estimation. The forward difference method is used to approximate the time derivatives in order to discretize the model in equation (3). The first step in the process is

$$\frac{R(k+1) - R(k)}{\Delta} = [R(k) + \alpha(k)]\beta(k). \tag{4}$$

Solving for $R(k+1)$ and applying the method to $\dot{\alpha}$ and $\dot{\beta}$ we get:

$$\begin{aligned} R(k+1) &= R(k) + \Delta t\beta(k)[R(k) + \alpha(k)], \\ \alpha(k+1) &= \alpha(k), \\ \beta(k+1) &= \beta(k). \end{aligned} \tag{5}$$

4 PROGNOSTICS ALGORITHM DEVELOPMENT

A prognostics algorithm in this application predicts the remaining useful life of a particular power MOSFET device at different points in time through the accelerated life of the device. As indicated earlier, $\Delta R_{DS(ON)}$ is used in this study as a health indicator feature and as a precursor of failure. The prognostics problem is posed in the following way.

- A single feature is used to assess the health state of the device ($\Delta R_{DS(ON)}$).
- It is assumed that the die-attached failure mechanism is the only active degradation during the accelerated aging experiment.
- Furthermore, $\Delta R_{DS(ON)}$ accounts for the degradation progression from nominal condition through failure.
- Periodic measurements with fixed sampling rate are available for $\Delta R_{DS(ON)}$.
- A crisp failure threshold of 0.045 in $\Delta R_{DS(ON)}$ is used.
- The prognostics algorithm will make a prediction of the remaining useful life at time t_p, using all the measurements up to this point either to estimate the health state at time t_p in a Bayesian tracking framework.

4.1 Extended Kalman filter implementation

Extended Kalman filter allows for the implementation of the Kalman filter algorithm for on-line estimation on non-linear dynamic systems [13, 14]. This algorithm has been used in other applications for health state estimation and prognostics. The general form of extended Kalman filter is given as;

$$\begin{aligned} x(k+1) &= \vec{f}\big(x(k), u(k)\big) + w(k), \\ y(k) &= h\big(x(k)\big) + v(k), \end{aligned} \tag{6}$$

where f and h are non-linear equations, $w(k)$ is the model noise and $v(k)$ is the measurement noise. Noise is considered to be normally distributed, with zero mean and known variance Q and R for $w(k)$ and $v(k)$ respectively.

For the prognostics implementation using the discrete dynamic degradation model in equation (5), the state variable is defined as

$$x(k) = \{x_1(k), x_2(k),\ x_3(k)\} = \{R(k), \alpha(k), \beta(k)\}. \quad (7)$$

Therefore, f is a vector valued function given by equation (8). The ON-resistance is the only measured value; therefore, the measurement equation h is given by equation (9).

$$\vec{f} = \begin{bmatrix} x_1(k) + \Delta x_2(k)[x_1(k) + x_3(k)] \\ x_2(k) \\ x_3(k) \end{bmatrix} \quad (8)$$

$$h = x_1(k) \quad (9)$$

5 RUL ESTIMATION RESULTS

This section presents the results of the algorithm implemented. Four test cases are defined as follows following the leave one out validation concept:

- T_1: Predict RUL on device #36, estimate initial conditions with the rest of the devices and compute RUL at times $t_p = [140,150,160,170,180,190,195,200,205,210]$
- T_2: Predict RUL on device #09, estimate initial conditions with the rest of the devices and compute RUL at times $t_p = [140,150,160,170,180,190,195,200,205,210]$
- T_3: Predict RUL on device #08, estimate initial conditions with the rest of the devices and compute RUL at times $t_p = [80, 90,100,110,120,125,130,135,140]$
- T_4: Predict RUL on device #14, estimate initial conditions with the rest of the devices and compute RUL at times $t_p = [80, 90,100,110,120,125,130,135,140]$

RUL estimates are computed by subtracting the time when the prediction was made from the time when predicted R crosses the failure threshold. As more data becomes available, the predictions are expected to become more accurate and more precise. Table 2 presents the initial conditions for all the test cases. The initial conditions for the parameters and their corresponding variances are computed by taking the sample mean and sample standard deviation of training device parameters in Table 1. The initial value for R and its standard deviation, are computed by using the first ten data points in the training devices.

Test	$\hat{\alpha}_O$	$\hat{\sigma}_\alpha$	$\hat{\beta}_O$	$\hat{\sigma}_\beta$	$\hat{R}_O$	$\hat{\sigma}_R$
T_1	$2.6\text{x}10^{-4}$	$3.2\text{x}10^{-4}$	$3.5\text{x}10^{-2}$	$1\text{x}10^{-2}$	$3.8\text{x}10^{-5}$	$2.4\text{x}10^{-3}$
T_2	$2.6\text{x}10^{-4}$	$1.1\text{x}10^{-3}$	$3.5\text{x}10^{-2}$	$1\text{x}10^{-2}$	$3.9\text{x}10^{-5}$	$2.2\text{x}10^{-3}$
T_3	$2.6\text{x}10^{-4}$	$1.1\text{x}10^{-3}$	$3.5\text{x}10^{-2}$	$1\text{x}10^{-2}$	$3.8\text{x}10^{-5}$	$2.3\text{x}10^{-3}$
T_4	$3.7\text{x}10^{-4}$	$1.1\text{x}10^{-3}$	$3.2\text{x}10^{-2}$	$1\text{x}10^{-2}$	$3.8\text{x}10^{-5}$	$2.6\text{x}10^{-3}$

Table 2. Initial conditions for the state vector and its corresponding variance for all the test cases.

Figure 3 and Figure 4 present the RUL estimation results for test cases T_1 and T_3 respectively. Analysis of the subplots from top to bottom shows how the prediction progresses as more data becomes available and the device gets closer to end of life. It also describes how prognostics consists of periodic RUL predictions through the life of the device.

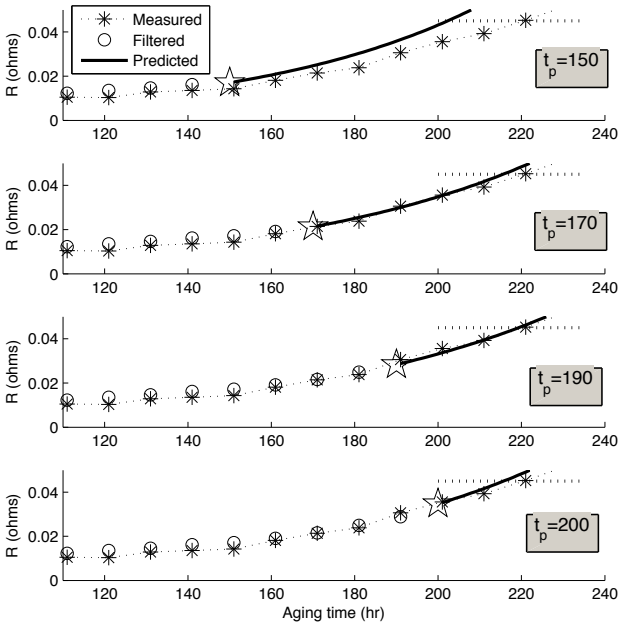

Figure 3. Health state ($\Delta R_{DS(ON)}$) tracking and RUL forecasting for test case T_1.

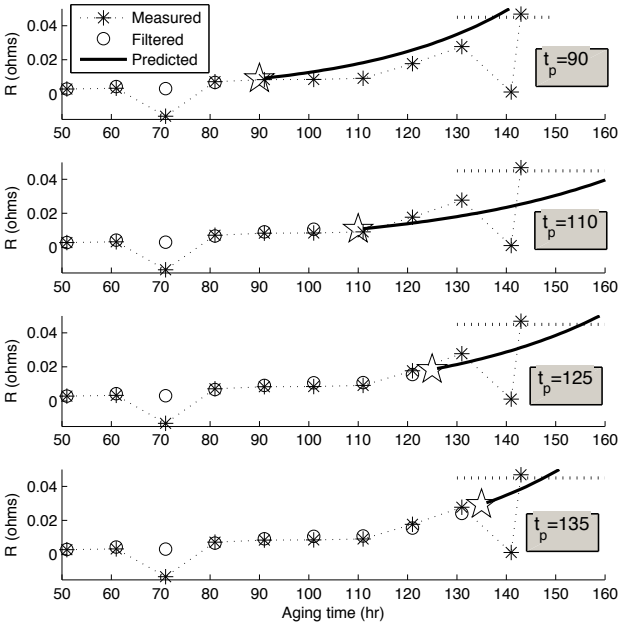

Figure 4. Health state ($\Delta R_{DS(ON)}$) tracking and RUL forecasting for test case T_3.

Table 3 and Table 4 present the state estimation results for $\Delta R_{DS(ON)}$ and the forecasting of $\Delta R_{DS(ON)}$ after measurements are no longer available. Measurements are available up to time t_p, these are use by the algorithm to adjust the estate estimation. The prediction portion starts after t_p. An estimate of the expected value of RUL is presented along with the sample standard deviation. These values are computed by Monte Carlo simulation using the last available state estimate and the state transition equation in (8). The estimation error and relative accuracy (RA) are presented as performance metrics. RA is defined as

$$RA \stackrel{\text{def}}{=} 100\left(1 - \frac{|RUL^* - RUL'|}{RUL^*}\right). \quad (10)$$

t_p	T_1			T_2		
	RUL (σ_{RUL})	Error	RA	RUL (σ_{RUL})	Error	RA
140	49.545 (1.180)	30.583	61.840	61.707 (1.598)	26.212	70.181
150	52.260 (1.297)	17.817	74.600	55.237 (1.306)	22.649	70.928
160	50.275 (1.249)	9.862	83.602	46.184 (1.011)	21.744	67.978
170	45.548 (1.129)	4.590	90.847	35.619 (0.682)	22.266	61.546
180	37.342 (1.001)	2.802	93.020	27.040 (0.548)	20.857	56.461
190	29.265 (0.816)	0.889	97.052	21.319 (0.479)	16.578	56.263
195	21.336 (0.646)	3.757	85.058	19.548 (0.466)	13.339	59.462
200	15.673 (0.517)	4.476	77.781	16.983 (0.430)	10.900	60.936
205	10.953 (0.427)	4.198	72.280	14.169 (0.389)	8.730	61.886
210	6.608 (0.314)	3.523	65.272	11.737 (0.359)	6.161	65.587

Table 3. RUL estimation results for test cases T_1 and T_2. The mean RUL and the standard deviation are presented in the first column; error and relative accuracy are presented in the second and third column of each test case.

t_p	T_3			T_4		
	RUL (σ_{RUL})	Error	RA	RUL (σ_{RUL})	Error	RA
80	56.166 (1.461)	6.379	89.816	56.180 (1.391)	7.162	88.704
90	47.521 (1.018)	5.117	90.277	53.680 (1.247)	-0.262	99.510
100	46.605 (0.984)	-4.001	90.616	61.609 (1.520)	-18.218	58.026
110	54.881 (1.237)	-22.329	31.573	65.075 (1.757)	-31.798	4.807
120	40.287 (0.858)	-17.631	22.100	47.704 (1.045)	-24.304	-3.847
125	30.310 (0.586)	-12.666	28.168	36.258 (0.781)	-17.885	2.818
130	21.614 (0.402)	-8.999	28.766	24.550 (0.493)	-11.160	16.737
135	12.615 (0.238)	-4.996	34.539	13.499 (0.272)	-5.078	39.577
140	5.795 (0.141)	-3.162	-20.125	6.599 (0.168)	-3.197	6.081

Table 4. RUL estimation results for test cases T_3 and T_4. The mean RUL and the standard deviation are presented in the first column; error and relative accuracy are presented in the second and third column of each test case.

The performance of the algorithm depends on the selection of the covariance matrix Q for the model noise $w(k)$ and the variance R for the measurement noise $v(k)$. Their respective values have been used as tuning parameters for the algorithm. The covariance values were constant for all the tests cases.

$$Q = \begin{bmatrix} 7.4\times10^{-9} & 0 & 0 \\ 0 & 7.4\times10^{-9} & 0 \\ 0 & 0 & 7.4\times10^{-9} \end{bmatrix}$$
$$R = 0.0001$$

REFERENCES

1. Celaya, J.R., A. Saxena, S. Saha, and K. Goebel, "Prognostics of Power MOSFETs under Thermal Stress Accelerated Aging using Data-Driven and Model-Based Methodologies", in *Annual Conference of the Prognostics and Health Management Society*2011.
2. Saha, B., J.R. Celaya, P.F. Wysocki, and K.F. Goebel. "Towards prognostics for electronics components". in *Aerospace conference, 2009 IEEE*. 2009.
3. Saha, S., J.R. Celaya, V. Vashchenko, S. Mahiuddin, and K.F. Goebel. "Accelerated Aging with Electrical Overstress and Prognostics for Power MOSFETs". in *IEEE EnergyTech 2011*. 2011.
4. Patil, N., J. Celaya, D. Das, K. Goebel, and M. Pecht, "Precursor Parameter Identification for Insulated Gate Bipolar Transistor (IGBT) Prognostics". *IEEE Transactions on Reliability*, 2009. **58**(2): p. 276.
5. Sonnenfeld, G., K. Goebel, and J.R. Celaya. "An agile accelerated aging, characterization and scenario simulation system for gate controlled power transistors". in *IEEE AUTOTESTCON 2008*. 2008.
6. Brown, D., M. Abbas, A. Ginart, I. Ali, P. Kalgren, and G. Vachtsevanos. "Turn-off Time as a Precursor for Gate Bipolar Transistor Latch-up Faults in Electric Motor Drives". in *Annual Conference of the Prognostics and Health Management Society 2010*. 2010.
7. Ginart, A., M. Roemer, P. Kalgren, and K. Goebel. "Modeling Aging Effects of IGBTs in Power Drives by Ringing Characterization". in *IEEE International Conference on Prognostics and Health Management*. 2008.
8. Celaya, J., A. Saxena, P. Wysocki, S. Saha, and K. Goebel. "Towards Prognostics of Power MOSFETs: Accelerated Aging and Precursors of Failure". in *Annual Conference of the Prognostics and Health Management Society 2010*. 2010.
9. Celaya, J.R., N. Patil, S. Saha, P. Wysocki, and K. Goebel. "Towards Accelerated Aging Methodologies and Health Management of Power MOSFETs (Technical Brief)". in *Annual Conference of the Prognostics and Health Management Society 2009*. 2009.
10. Celaya, J.R., P. Wysocki, V. Vashchenko, S. Saha, and K. Goebel. "Accelerated aging system for prognostics of power semiconductor devices". in *2010 IEEE*

AUTOTESTCON. 2010.
11. Ginart, A.E., I.N. Ali, J.R. Celaya, P.W. Kalgren, S.D. Poll, and M.J. Roemer. "Modeling SiO2 Ion Impurities Aging in Insulated Gate Power Devices Under Temperature and Voltage Stress". in *Annual Conference of the Prognostics and Health Management Society 2010*. 2010.
12. Celaya, J., C. Kulkarni, G. Biswas, and K. Goebel. "Towards Prognostics of Electrolytic Capacitors". in *AIAA Infotech@Aerospace*. 2011. St. Louis, MO.
13. Rasmussen, C.E. and C.K.I. Williams, "Gaussian Processes for Machine Learning"2006. MIT Press.
14. Meinhold, R.J. and N.D. Singpurwalla, "Understanding the Kalman Filter". *The American Statistician*, 1983. **37**(2): p. 123-127.

BIOGRAPHIES

José R. Celaya, PhD
NASA Ames Research Center (SGT Inc.)
Prognostics Center of Excellence
MS 269-4
Moffett Field, CA 94035, USA

email: jose.r.celaya@nasa.gov

José R. Celaya is a research scientist with SGT Inc. at the Prognostics Center of Excellence, NASA Ames Research Center. He received a PhD degree in Decision Sciences and Engineering Systems in 2008, a M. E. degree in Operations Research and Statistics in 2008, a M. S. degree in Electrical Engineering in 2003, all from Rensselaer Polytechnic Institute, Troy New York; and a B. S. in Cybernetics Engineering in 2001 from CETYS University, México.

Abhinav Saxena, PhD
NASA Ames Research Center (SGT Inc.)
Prognostics Center of Excellence
MS 269-4
Moffett Field, CA 94035, USA

email: abhinav.saxena@nasa.gov

Abhinav Saxena is a Research Scientist with SGT Inc. at the Prognostics Center of Excellence NASA Ames Research Center, Moffett Field CA. His research focus lies in developing and evaluating prognostic algorithms for engineering systems using soft computing techniques. He is a PhD in Electrical and Computer Engineering from Georgia Institute of Technology, Atlanta. He earned his B.Tech in 2001 from Indian Institute of Technology (IIT) Delhi, and Masters Degree in 2003 from Georgia Tech. Abhinav has been a GM manufacturing scholar and is also a member of IEEE, AAAI and ASME.

Chetan Kulkarni
ISIS, Vanderbilt University
1025 16th Avenue
Nashville, TN, 37212, USA

email: chetan.kulkarni@vanderbilt.edu

Chetan S Kulkarni is a Research Assistant at ISIS, Vanderbilt University. He received the M.S. degree in EECS from Vanderbilt University, Nashville, TN, in 2009, where he is currently a PhD student.

Sankalita Saha, PhD
NASA Ames Research Center (MCT)
Prognostics Center of Excellence
MS 269-4
Moffett Field, CA 94035, USA

email: sankalita.saha@nasa.gov

Sankalita Saha is a research scientist with Mission Critical Technologies at the Prognostics Center of Excellence, NASA Ames Research Center. She received the M.S. and PhD degrees in Electrical Engineering from University of Maryland, College Park in 2007. Prior to that she obtained her B.Tech (Bachelor of Technology) degree in Electronics and Electrical Communications Engineering from the Indian Institute of Technology, Kharagpur in 2002.

Kai Goebel, PhD
NASA Ames Research Center
Prognostics Center of Excellence
MS 269-1
Moffett Field, CA 94035, USA

email: kai.goebel@nasa.gov

Kai Goebel received the degree of Diplom-Ingenieur from the Technische Universitt Mnchen, Germany in 1990. He received the M.S. and PhD from the University of California at Berkeley in 1993 and 1996, respectively. Dr. Goebel is a senior scientist at NASA Ames Research Center where he leads the Diagnostics and Prognostics groups in the Intelligent Systems division. In addition, he directs the Prognostics Center of Excellence and he is the technical lead for Prognostics and Decision Making of NASA's System-wide Safety and Assurance Technologies Program. He worked at General Electric's Corporate Research Center in Niskayuna, NY from 1997 to 2006 as a senior research scientist. He has carried out applied research in the areas of artificial intelligence, soft computing, and information fusion. His research interest lies in advancing these techniques for real time monitoring, diagnostics, and prognostics. He holds 15 patents and has published more than 200 papers in the area of systems health management.